Uniformly oriented, ellipsoidal nanovoids in glass created by electric-field-assisted dissolution of metallic nanoparticles

M. Leitner,* H. Peterlik, and B. Sepiol
Fakultät für Physik, Universität Wien, Strudlhofgasse 4, A-1090 Wien, Austria

H. Graener, M. Beleites, and G. Seifert
Institut für Physik, Martin-Luther-Universität Halle-Wittenberg, D-06099 Halle, Germany
(Received 22 July 2008; revised manuscript received 27 March 2009; published 24 April 2009)

Nanoporous glass containing spherical or ellipsoidal nanovoids, respectively, has been produced by electric-field-assisted dissolution of Ag nanoparticles embedded in glass-metal nanocomposites. Small angle x-ray scattering before and after particle dissolution gives evidence that in the case of spherical nanoparticles the remaining nanovoids have the same size distribution (≈20 nm average diameter) as the original silver particles. Spheroidal particles of uniform orientation leave strongly aspherical nanovoids, which undergo a slight shape relaxation from aspect ratio 4.7 (particles) to 3.8 (holes).

DOI: 10.1103/PhysRevB.79.153408 PACS number(s): 81.07.−b, 78.67.−n, 81.05.Rm, 61.05.cf

Micro- and nanostructuring, often by ultrashort laser pulses, are widely used approaches to control the optical properties of glass-based materials.[1–8] Recently we demonstrated that Ag nanoparticles included in glass-metal nanocomposites may disappear after treating the material with a combination of a moderately high dc voltage (≈1 kV) and elevated temperature (≈280 °C).[9] This process was termed "electric-field-assisted dissolution" (EFAD), because the silver from the destroyed nanoparticles is dissolved in the glass in form of Ag^+ ions.[10] Already the first studies of this effect gave strong hints that the depleted layer remains nanoporous.[10,11] Recently Lipovskii *et al.*[12] showed electron microscope images suggesting holes after EFAD in the anodic surface of samples with a very thin layer (≈200 nm) containing silver nanoparticles at relatively high volume concentration up to 10%. Also, field-dependent surface imprints have been reported.[12] This study, however, did not provide any quantitative information about size, shape, or concentration of holes. Thus, it is an open question if each dissolved nanoparticle leaves a corresponding hollow space after EFAD, or if the procedure leads to shape relaxation and/or collapsing of the voids.

In this Brief Report, we present a small angle x-ray scattering (SAXS) study aiming to answer this open question. Using samples with low particle concentrations (representing the limit of noninteracting nanoparticles) and comparing the scattered x-ray intensity before and after electric-field-assisted dissolution of spherical and ellipsoidal Ag nanoparticles, we can clearly show that nanovoids, typically of the same volume and shape as the particles are, remain after EFAD. In particular, we will show that in the case of a sample containing uniformly oriented silver nanospheroids, the dissolution process leaves also uniformly oriented spheroidal nanovoids, with an only slightly smaller aspect ratio compared to that of the original Ag particles.

The samples for this study were prepared from soda-lime float glass (72.5 SiO_2, 14.4 Na_2O, 0.7 K_2O, 6.1 CaO, 4.0 MgO, 1.5 Al_2O_3, 0.1 Fe_2O_3, 0.1 MnO, 0.4 SO_3 in wt %) by Ag^+-Na^+ ion exchange in a mixed melt of $AgNO_3$ and KNO_3 at 400 °C. By subsequent annealing in a H_2 reduction atmosphere at typically 400–450 °C spherical silver nanoparticles are formed in a thin subsurface layer. Sizes and spatial distribution of the Ag clusters can be controlled by the processing parameters (mainly by the sequence of temperature and timing).[8,10] For this study we used two types of samples: the first type contains spherical particles with mean diameter of ≈20 nm in a surface layer of ≈10 μm thickness (concluded from a sample cross section by microscope spectrometry). The average Ag volume content in this layer is in the range of 4×10^{-3} (estimated from optical absorption and SAXS intensity, see below). Figure 1(a) shows an optical-absorption spectrum of the sample (dashed line) with a very strong surface-plasmon resonance absorption around 420 nm (optical density $OD=\log_{10}(T)>10$; T: intensity transmission). For the second type of samples a further step of processing was performed: these samples were stretched by tensile deformation and simultaneous heating to the glass transition temperature (≈600 °C), transforming the original layer of spherical nanoparticles into a near-surface layer of

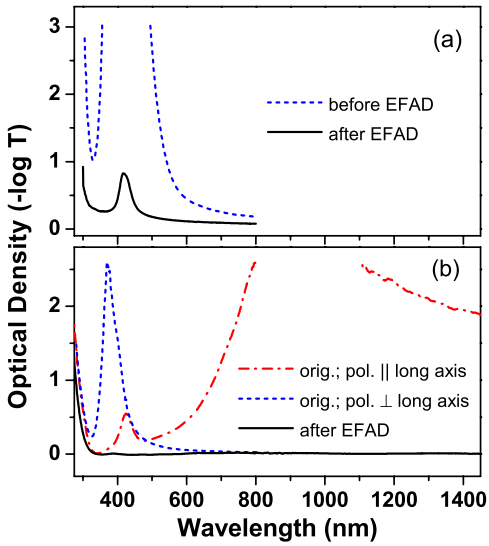

FIG. 1. (Color online) Absorption spectra of samples before and after EFAD; (a) spherical, (b) ellipsoidal Ag particles.

≈ 1 μm thickness containing elongated (ellipsoidal) nanoparticles of uniform orientation.[13] Due to this deformation, the surface-plasmon resonance splits into two polarization-dependent absorption bands: as shown in Fig. 1(b), for light polarized parallel to the long particle axis a broad absorption band with optical density >3 around 900 nm is observed, whereas light polarized parallel to the short particle axes experiences a smaller absorption band centered at 370 nm ($OD_{max} \approx 2.6$). The latter allows an estimation of the silver content from the well-known absorption cross sections of Ag nanoparticles,[14,15] yielding again a silver volume fill factor of $\approx 4 \times 10^{-3}$. This is consistent with the fact that the stretching does not change the width-to-thickness ratio of the sample.

These samples were then equipped with two steel electrodes pressed onto the surfaces, the anode facing the layer containing nanoparticles. For complete dissolution the samples were heated to a temperature of 280 °C, and a dc voltage was stepwise increased up to a maximum value of 1 kV (sample with ellipsoidal particles) or 3 kV (sample with spherical particles), respectively. The total treatment time was about 1 h. The voltage steps have to be chosen such that the electrical current is limited to 250 μA to avoid the degrading electric breakdown of the material. After that procedure the region under the anode has turned from originally brown to faint yellow (type 1) or, respectively, from dark green to transparent (type 2).[8] This could be quantified by optical spectroscopy: the solid curves in Fig. 1 refer to the absorption spectra from the bleached regions, where clearly the plasmon resonance absorption of the metal nanoparticles has vanished [Fig. 1(b)] or at least decreased dramatically [Fig. 1(a)]. From the remaining absorption ($OD_{max} \approx 0.5$) seen in Fig. 1(a) we can conclude that less than 1% of the original amount of Ag nanoparticles is still present (or was reformed in a deeper layer) in samples of type 1 after the EFAD procedure.

Previous studies [scanning electron microscopy (SEM), photoluminescence] have shown that the silver of the destroyed particles is still within the glass in the form of ions, which however do not absorb light in the visible range. These Ag^+ ions are located in regions further away from the surface,[10] the distance depending on voltage and processing time. In previous work there have been seen also some indications of nanovoids, e.g., dark spots in SEM images,[10] or the need for a subsurface layer with lowered refractive index to explain optical reflection spectra of partially bleached samples.[11]

In order to prove the existence of nanovoids after particle dissolution, we have conducted small-angle x-ray scattering in both bleached and unchanged regions of the samples. As x-ray source a rotating anode generator (Bruker Nanostar) with a wavelength of 0.154 nm (Cu-Kα radiation), a pinhole camera with a beam monochromatized from crossed Göbel mirrors and a beam width of 0.5 mm at the sample was used. The scattered intensity was recorded with a two-dimensional (2D) position sensitive detector (Vantec 2000, gas detector with microgap technology).

The samples were ground down to a thickness of 200 μm and measured in transmission geometry. The absorption length of the glass was 102 μm, corresponding to a transmission of 14%.

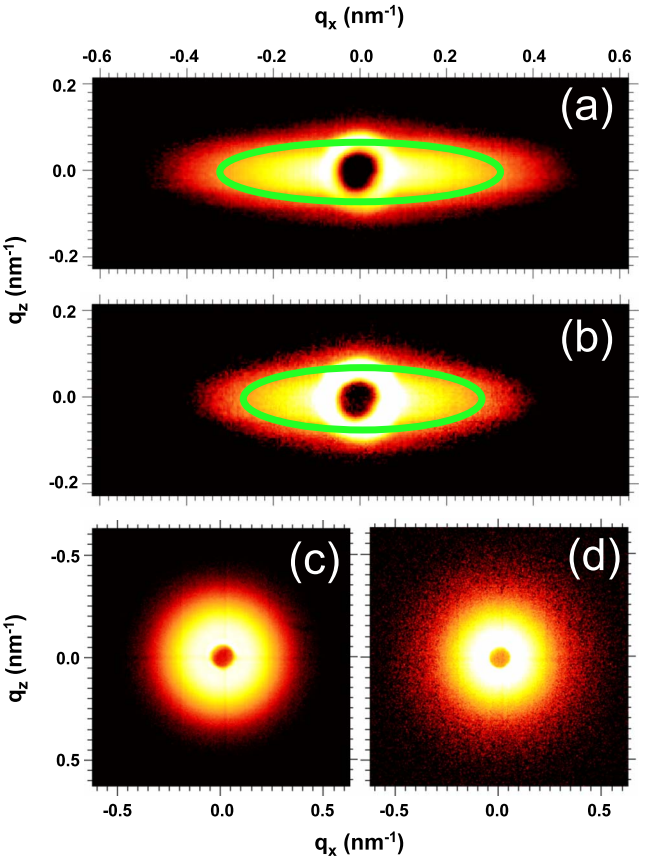

FIG. 2. (Color online) Details of the SAXS signal in a logarithmic false-color/grayscale representation: Elongated particles both before (a) and after (b) EFAD. The aspect ratio of the superimposed ellipse is 4.7 in (a) and 3.8 in (b). Spherical particles both before (c) and after (d) EFAD. The color scales/grayscales of (c) and (d) differ by a factor of 15. The central dark spot and the bright ring around it are the shadow of the beam stop and parasitic scattering from the apertures, respectively.

Figure 2 shows the 2D SAXS signal obtained from a sample containing uniformly oriented spheroidal Ag nanoparticles, both before [Fig. 2(a)] and after [Fig. 2(b)] EFAD. A full quantitative evaluation in this case is not possible, as the information concerning the long particle axis is hidden under the parasitic scattering, so we concentrate on the anisotropy of the signals, which is the inverse of the aspect ratio of the scattering objects. Clearly the anisotropic signal before EFAD [Fig. 2(a)] is due to the Ag spheroids. By fitting an ellipse to the data, a mean aspect ratio of the particles of $c/a \approx 4.7$ is found in accordance with the optical absorption. After EFAD a weaker signal with a reduced aspect ratio of ≈ 3.8 is visible. Since the optical absorption has vanished after EFAD [Fig. 1(b)], clearly no more Ag particles are present. Assuming that for each destroyed particle a nanohole with the same volume is left in the glass, a similar signal as before EFAD, but with reduced intensity can be expected due to the different electron-density differences between silver and glass and between glass and vacuum, respectively (see below). Thus our SAXS results on the mechanically stretched nanocomposites clearly prove the existence of ellipsoidal nanovoids, which have experienced a

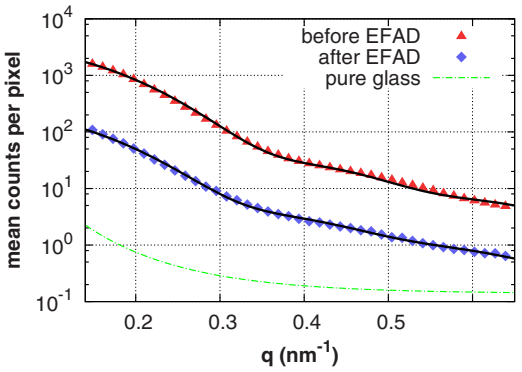

FIG. 3. (Color online) Scattered intensity as function of modulus of scattering vector q both before (upper curve) and after EFAD (lower curve) together with fits as explained in the text, also background due to the glass matrix. Exposure time was 11 h.

moderate shape change during the EFAD process.

The SAXS results obtained on the samples containing initially spherical nanoparticles [Fig. 2(c) and 2(d)] are not dominated by parasitic scattering in the interesting q range, and thus can be interpreted quantitatively by a more detailed analysis. Neglecting absorption, the scattered intensity per steradian of a population $p(R)$ of spheres is given by[16]

$$I(q) = nI_0(r_0\Delta\rho)^2 \int \mathrm{d}Rp(R)\left(3V\frac{\sin(x) - x\cos(x)}{x^3}\right)^2. \quad (1)$$

Here x is an abbreviation for qR, r_0 is the Thomson electron radius, V is the volume of the particle, $\Delta\rho$ is the difference in electron density between particle and surrounding matrix, n the number of particles per area and I_0 the incident radiation. Adding the intensities incoherently, that is, neglecting correlations between the positions of the scatterers, is valid due to the low volume fill factors of the particles.

Figure 3 shows the pertinent intensities recorded as a function of modulus of scattering vector q. First, the scattering of a pure glass sample was measured. For fitting the spectra of the samples both before and after EFAD, this properly rescaled background was added to Eq. (1). The fit of the scattered intensity before EFAD yields a mean particle radius of $R_1 = (9.9 \pm 0.1)$ nm with a width of the distribution $\sigma_1 = (2.7 \pm 0.1)$ nm. The area density of particles can be computed from Eq. (1), using the fitted prefactor, the known incident intensity of 1.9×10^7 s^{-1}, and the solid angle of a pixel $(3.665 \times 10^{-9}$ sr); taking finally absorption in the sample into account, a value of $n = 7.5 \times 10^{-3}$ nm^{-2} is obtained. Together with the size of the particles and the layer thickness this translates to a volume fill factor of 0.4%, in accordance with the optical absorption.

After EFAD, the scattered intensity has decreased by a factor of 15, while the average particle radius and distribution width remain approximately constant, namely, $R_2 = (10.1 \pm 0.1)$ nm and $\sigma_2 = (3.0 \pm 0.1)$ nm. In order to fit the spectrum, though, additionally a distribution centered around 3 nm has to be added. This additional contribution is very weak, so its parameters are very poorly defined. The physical interpretation of this background is not really clear; possible explanations would be the onset of surface destruction by

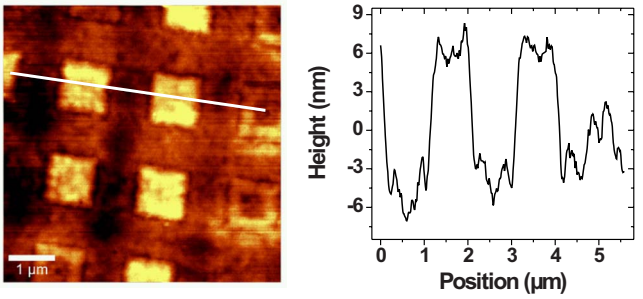

FIG. 4. (Color online) AFM image of sample surface after EFAD with a microstructured electrode.

way of ion depletion as reported in Ref. 12 or, more generally, additional defects in the glass matrix caused by removal of ions from the subsurface layer by the static electric field.

The decrease in scattered intensity can only partially be explained by the electron-density differences of silver in glass to a void in glass: according to Eq. (1), intensity scales with $\Delta\rho^2$. As $(\rho_{\mathrm{Ag}} - \rho_{\mathrm{Gl}})/(0 - \rho_{\mathrm{Gl}}) = -2.76$, the observed intensity difference exceeds the expectation from the different electron densities by a factor of 2, indicating that half of the volume of the scatterers (voids) is lost compared to the total particle volume before EFAD. Since the average radius of particles and voids is equal $(R_1 = R_2)$ within experimental accuracy, it can be concluded that only $\approx 50\%$ of the voids survive the procedure, while the other half are collapsing or being refilled. Possible mechanisms will be discussed below. In any case, however, this effect lets one expect a volume shrinking of the bleached regions. Regarding the layer thickness of ≈ 10 μm and the initial Ag particle concentration of $\approx 4 \times 10^{-3}$, an imprint of ≈ 20 nm is estimated.

Since it is almost impossible to monitor such a small height difference over a macroscopic surface area (the electrode was ≈ 1 cm^2), we bleached another sample of type 1 using a microstructured electrode (Si photonic crystal with a 2 μm square lattice),[17] and analyzed the resulting surface profile by atomic force microscopy (AFM). A typical result is shown in Fig. 4: the image on the left-hand side represents the surface topology of a $\approx 6 \times 6$ μm^2 square area in the microstructured, bleached region, clearly demonstrating the imprint of the electrode (darker regions); the height profile along the white line in this image is given separately in the graph on the right-hand side. Analyzing several such spots within the bleached area, we found in each case height steps in the range of 8–20 nm separating the elevated squares from the imprinted grid. These numbers are well compatible with the volume loss of the nanovoids estimated above.

It is an interesting question to discuss which processes on the nanoscale are responsible for the electric-field nanoimprinting of the sample surface. Lipovskii *et al.*[12] proposed two main mechanisms: the first one is relaxation of internal stresses in the glass due to the smaller volume of Ag ions in glass[18] compared to Ag atoms,[19] the second one is field-driven ion migration of alkaline (in particular the most mobile Na^+) and calcium ions, which can produce an ion-depleted subsurface layer of a few microns.[20] This so-called poling of glass appears to be the more important point considering our SAXS results: by internal stress relaxation alone

the holes should shrink upon Ag nanoparticle dissolution, but their number should remain constant. Instead, the fitted parameters do not show a change in the size distributions of particles (before EFAD) and voids (after EFAD), but a significant decrease in number density after EFAD. This favors a scenario of ions diffusing away from the anode, which in deeper regions of the initial sample layer containing Ag nanoparticles can be incorporated into the glass matrix due to the available space, thereby causing the voids to gradually become compressed. Depending on initial size and time, this may lead to complete refilling (collapsing) of part of the voids. In contrast, in the subsurface region where ions are being removed in a very early stage of the EFAD process, the voids should keep their original size or even grow a little bit as a reaction to shrinking of the ion-depleted glass matrix. These opposite effects in the subsurface or deeper sample layers might balance each other with respect to the average radius of particles and voids. More detailed future work, e.g., studying different nanoparticle size distributions, will be necessary to clear this, at the moment rather speculative, point.

Finally, it should be mentioned that the SAXS results on the samples containing spheroidal particles or voids are also supporting the above interpretation. In this case the scattering intensities before and after EFAD correspond quite well to the expectation from the electron-density difference, i.e., there is no indication for hole refilling. The particle-containing layer of these samples was only ≈ 1 μm thick. So the aforementioned glass poling will deplete the upper ≈ 1 μm layer comparably fast from mobile ions, tentatively even before the Ag particle dissolution starts—the strong increase in the static electric field upon ion depletion has been discussed as a crucial point to initiate the ionization and dissolution of Ag nanoparticles at all.[9,10] So the decrease in the voids' aspect ratio compared to that of the Ag particles can be understood as a nanoscopic relaxation of the hole shape toward the minimum surface energy, mediated by atomic diffusion on the inner surface of the voids, which seems plausible given the elevated temperature.

In conclusion, we have shown that both ellipsoidal and spherical nanovoids in glass can be prepared by electric-field-assisted dissolution of silver nanoparticles. The aspherical holes show a slight relaxation toward smaller aspect ratios. The spherical voids have the same average radii as the original Ag particles, but their number (i.e., total volume) is reduced by a factor of 2 in a comparably thick layer of 10 μm. This $\approx 50\%$ volume loss from Ag nanoparticles to voids, together with observed surface imprints of 8–20 nm indicate partial refilling of these holes during the EFAD processing by field-driven, migrating alkaline and calcium ions, with increasing probability for hole filling in larger distance from the anodic surface. In general, size, shape, and orientation of metal nanoparticles in glass are mostly transferred to the nanovoids produced by EFAD. So the results presented here show a technique to create nanoporous glass with controllable properties of the nanovoids.

ACKNOWLEDGMENTS

The authors thank CODIXX AG for the samples, and SFB 418 for financial support. M.L. acknowledges the support by the IC "Experimental Materials Science—Nanostructured Materials," a college for Ph.D. students at the University of Vienna.

*michael.leitner@univie.ac.at

[1] V. M. Shalaev, *Optical Properties of Nanostructured Random Media* (Springer, Berlin, 2001).
[2] P. Chakraborty, J. Mater. Sci. **33**, 2235 (1998).
[3] R. Jin, Y. W. Cao, C. A. Mirkin, K. L. Kelly, G. C. Schatz, and J. G. Zheng, Science **294**, 1901 (2001).
[4] T. Wenzel, J. Bosbach, A. Goldmann, F. Stietz, and F. Träger, Appl. Phys. B: Lasers Opt. **69**, 513 (1999).
[5] F. Stietz, Appl. Phys. A **72**, 381 (2001).
[6] A. L. Stepanov and V. N. Popok, Surf. Coat. Technol. **185**, 30 (2004).
[7] M. Kaempfe, T. Rainer, K.-J. Berg, G. Seifert, and H. Graener, Appl. Phys. Lett. **74**, 1200 (1999).
[8] A. Podlipensky, A. Abdolvand, G. Seifert, and H. Graener, Appl. Phys. A **80**, 1647 (2005).
[9] O. Deparis, P. G. Kazansky, A. Abdolvand, A. Podlipensky, G. Seifert, and H. Graener, Appl. Phys. Lett. **85**, 872 (2004).
[10] A. Podlipensky, A. Abdolvand, G. Seifert, H. Graener, O. Deparis, and P. G. Kazansky, J. Phys. Chem. B **108**, 17699 (2004).
[11] J. Sancho-Parramon, A. Abdolvand, A. Podlipensky, G. Seifert, H. Graener, and F. Syrowatka, Appl. Opt. **45**, 8874 (2006).
[12] A. A. Lipovskii, M. Kuittinen, P. Karvinen, K. Leinonen, V. G. Melehin, V. V. Zhurikhina, and Y. P. Svirko, Nanotechnology **19**, 415304 (2008).
[13] M. Suszynska, L. Krajczyk, R. Capelletti, A. Baraldi, and K. J. Berg, J. Non-Cryst. Solids **315**, 114 (2003).
[14] U. Kreibig and M. Vollmer, *Optical Properties of Metal Clusters* (Springer, Berlin, 1995).
[15] P. Billaud, J.-R. Huntzinger, E. Cottancin, J. Lermé, M. Pellarin, L. Arnaud, M. Broyer, N. D. Fatti, and F. Vallée, Eur. Phys. J. D **43**, 271 (2007).
[16] O. Glatter and O. Kratky, *Small Angle X-ray Scattering* (Academic Press, London, 1982).
[17] A. Abdolvand, A. Podlipensky, S. Matthias, F. Syrowatka, U. Gösele, G. Seifert, and H. Graener, Adv. Mater. **17**, 2983 (2005).
[18] J. L. Coutaz and P. C. Jaussaud, Appl. Opt. **21**, 1063 (1982).
[19] D. Yoder-Short, J. Appl. Crystallogr. **26**, 272 (1993).
[20] P. G. Kazansky, A. Kamal, and P. S. J. Russell, Opt. Lett. **18**, 693 (1993).